Food Chemistry: X 21 (2024) 101153

Contents lists available at ScienceDirect

Food Chemistry: X

journal homepage: www.sciencedirect.com/journal/food-chemistry-x

A promising *Artemisia capillaris* Thunb. Leaf proteins with high nutrition, applicable function and excellent antioxidant activity

Wen-Lu Wei, Wen-Jun Wang, Hui Chen, Su-Yun Lin, Qiu-Shui Luo, Jian-Ming Li, Jin Yan, Ling-Li Chen *

Jiangxi Key Laboratory of Natural Products and Functional Food, College of Food Science and Engineering, Jiangxi Agricultural University, Nanchang 330045, China

A R T I C L E I N F O

Keywords:
Artemisia capillaris Thunb. leaf protein
Nutritional quality
Functional properties
Structural characterization
In vitro digestibility
Antioxidant activity

A B S T R A C T

The nutritional and functional properties of leaf proteins is a decisive factor for their use in food. This work was aimed to extract defatted *Artemisia capillaris* Thunb. (ACD) leaf proteins (ACLP), and assess ACLP nutritional quality, functional properties and *in vitro* antioxidant activity, as well characterize the structure. ACLP had a balanced amino acid profile and high bioavailability (protein digestibility corrected amino acid score (PDCAAS) 99.29 %). Solubility, foaming capacity and emulsifying ability of ACLP correlated positively with pH. Water and oil holding capacity were increased with temperature. Gel electrophoresis shown the protein molecular size was mainly ~25 kDa, and random coil was the mainly secondary structure while β-sheet was dominant regular conformation as indicated by circular dichroism (CD). ACLP performed *in vitro* antioxidant activity which was better after digestion. All data implied ACLP met the WHO/FAO protein quality expectations and had application potential in food.

1. Introduction

Since the 19th century, a growing world population and the challenges of urbanization have driven the demand for rich and sustainable highly nutritious food (Sá, Moreno, & Carciofi, 2020). Due to health and environmental concerns, there has been a trend in recent years to replace animal proteins with plant proteins. Plant proteins have a major impact on human health and changing social demographics and are more environmentally sustainable. Green plants are one of the world's largest renewable resources with easy and low-cost access, representing a promising candidate for protein production (Sim, Srv, Chiang, & Henry, 2021). Except for the traditional plant protein from seeds, leaf proteins have gained increasing interest recently, not only for their richness in proteins and lack of cholesterol but also for some functional activity like antioxidant properties (Calderón-Chiu, Calderón-Santoyo, Herman-Lara, & Ragazzo-Sánchez, 2021).

In fact, recovering protein from leafy plants is not a new concept, research on this topic can be stretched back to the 1940s (Pirie, 1942), but has gained growing attention in recent decades for their huge potential as a sustainable protein source for food and feed. Leaf proteins are mainly extracted from the leaf and steam of green plant and finally formed as leaf protein concentrate, which typically obtains 40–60 % yield of the total leaf protein with large variation between species and extraction process (Hadidi et al., 2023). A number of different leafy plants can be used for the production of leaf protein, which can be mainly summarized into pasture (e.g., alfalfa, ryegrass), tree leaves (e.g., *Moringa Oleifera* leaves), agro-industrial by-products (e.g., sugar beet, broccoli) and other plant leaves (e.g., tobacco, bamboo leaves) (Pérez-Vila, Fenelon, O'Mahony, & Gómez-Mascaraque, 2022; Sá et al., 2020; Zhang, Grimi, Jaffrin, Ding, & Tang, 2017). Though many leaf proteins were demonstrated can provide high nutritional value proteins with enough essential amino acids (EAA) for human needs, such as Moringa Oleifera leaf protein (Benhammouche et al., 2021) and hemp protein isolate (Fang, Chang, Ohm, Chen, & Rao, 2023), their application as a new protein ingredient in the food was still scares. The most important reason is that leaf protein quality and functional properties are often inferior to animal proteins, and extraction processes also limit their industrialization. So, exploring various eminent leaf protein sources and deeply understanding the protein quality and functional properties is fundamental for their utilization in food.

Artemisia capillaris Thunb. (Named Yinchenhao in Chinese) (AC) belongs to the genus *Artemisia*, which is widely distributed in China, central Europe, Japan, India, North Korea, Mongolia, Russia, Poland, and so on (Cai, Zheng, Sun, Wu, Li, & Liu, 2020). AC is one of the earliest

* Correspondence author.
E-mail address: chenlingli89@163.com (L.-L. Chen).

https://doi.org/10.1016/j.fochx.2024.101153
Received 23 November 2023; Received in revised form 17 January 2024; Accepted 18 January 2024
Available online 21 January 2024

and most important edible indigenous herbs used for various medicinal purposes in Asian countries (Cai et al., 2020). Furthermore, AC is also a folk delicious wild vegetable eaten for thousands of years and is the key ingredient of the traditional snack "Qingming ba" in China. As one of the most commonly used herbs, AC has shown good results in the treatment of jaundice and liver diseases (Yang et al., 2023). However, research on AC has mainly focused on its efficacy and biological activity in medicine, while research on its nutritional role as food, especially on its protein is still scarce and remains a mystery. To our knowledge, no study has explored protein extraction from AC. Therefore, the objective of this work was to optimize the production of leaf protein from AC (ACLP) and to explore the protein quality, functional properties, structure, and antioxidant activity of ACLP. To attain this objective, commonly used alkaline extraction was applied and optimized using the response surface methodology (RSM) for the production of ACLP. And assessed the amino acid evaluation and protein digestibility corrected amino acid score (PDCAAS) of ACLP. Moreover, ACLP functional properties, structure, and antioxidant activity were investigated with biochemical assay and spectroscopy.

2. Materials and methods

2.1. Materials

2.1.1. Sampling and sample preparation

A composite sample of 5 kg AC was prepared in March 2022, by collecting leaves from ground level and above, which was purchased from suppliers in Haozhou County, Anhui Province, China. It was authenticated by Prof. Qingfeng Zhang at Jiangxi Agricultural University of Key Laboratory of Natural Products Research and Development, China. The collected plants were carefully screened to be ground with a grinder and sieved using a No. 60-mesh sieve, then defatted with petroleum ether (w/v 1:3) to obtain ACD for the production of protein concentrates. ACD was stored at room temperature in a desiccator for later use.

2.1.2. Reagents

Bicinchoninic Acid (BCA) Protein Assay Kit was purchased from Beyotime Biotechnology (Shanghai, China). Sodium dodecyl sulfate (SDS), glycine, urea, 5,5′-Dithiobis-(2-nitrobenzoic acid) (DTNB), and bile salts were purchased from Solarbio. (Beijing, China). Salivary amylase (12 U/mg), pepsin (3 U/mg), and Trypsin (250 U/mg) in pancreatin were obtained from Yuan Ye Biotechnology Corporation. (Shanghai, China). Potassium bromide was purchased from Macklin Biochemicals Co. (Shanghai, China). NaOH, HCl, Petroleum ether, Ethylene Diamine Tetraacetic Acid (EDTA), KCl, KH_2PO_4, $NaHCO_3$, NaCl, $MgCl_2$, $(NH_4)_2CO_3$, and $CaCl_2$ were purchased from Xilong Science Co. (Guangdong, China). All the other chemicals and reagents were of analytical grade and available commercially.

2.2. Methods

2.1.1. Optimization of protein extraction from ACD

ACD protein extraction was carried out using an alkaline extraction method. To increase the protein yield, four single-factor variables (material to liquid ratio; pH; temperature; time) affecting the extraction of plant proteins were optimized. The RSM method was optimized for ACLP extraction by reference to the method of Pasrija and Sogi (2022). Three key variables were selected based on the results of the single-factor experiment, and then the key variables were optimized using Box-Behnken Design (BBD).

Three important variables for BBD (material to liquid ratio; pH; temperature) were explored at 3 different levels (−1, 0, 1) (Table 1S). The optimized extraction conditions were confirmed based on the extracted protein yield (Table 2S). The ACLP was extracted using the optimized conditions: material to liquid ratio of 1:31, pH 11(1 M NaOH), extracted at 39 °C for 70 min under sonication (80 Hz). Then the soluble fraction was separated from the residual fraction by centrifugation (4000 rpm, 10 min). Next, the soluble fraction was adjusted to pH 4.0 (1 M HCl) and left overnight (4 °C) for isoelectric point precipitation. The

Table 1
Amino acid composition of ACD and ACLP with respect to the provisional scoring pattern of WHO/FAO.

Amino acid	WHO/FAO/UNU (2007)	ACD	ACD (AAS)	ACLP	ACLP (AAS)
His	15	18.13 ± 0.11	1.21 ± 0.01	33.89 ± 1.54	2.26 ± 0.1
Ile	30	45.83 ± 0.41	1.53 ± 0.01	45.29 ± 0.85	1.51 ± 0.03
Val	39	56.81 ± 0.83	1.46 ± 0.02	52.65 ± 0.71	1.35 ± 0.02
Asp		103.14 ± 0.96		94.76 ± 1.38	
Thr	23	49.38 ± 1.73	2.15 ± 0.08	58.43 ± 1.29	2.54 ± 0.06
Ser		44.09 ± 1.88		32.93 ± 1.14	
Leu	59	81.82 ± 1.81	1.39 ± 0.03	79.00 ± 0.58	1.34 ± 0.01
Tyr		39.73 ± 0.15		37.69 ± 0.22	
Lys	45	68.53 ± 0.56	1.52 ± 0.01	49.16 ± 0.75	1.09 ± 0.02
Arg		53.03 ± 0.52		60.59 ± 0.60	
Glu		125.26 ± 1.38		126.04 ± 1.24	
Gly		51.75 ± 0.47		52.78 ± 0.63	
Pro		76.67 ± 1.60		142.47 ± 1.84	
Met		2.13 ± 0.04		7.61 ± 0.66	
Ala		54.05 ± 0.68		49.41 ± 0.51	
Phe		45.91 ± 0.06		48.72 ± 0.23	
Trp	6	9.36 ± 0.20	1.56 ± 0.03	54.29 ± 1.34	9.05 ± 0.22
Cys		12.39 ± 0.18		14.24 ± 0.02	
∑AAA[1]	30	85.64 ± 0.22	2.85 ± 0.01	86.41 ± 0.02	2.88 ± 0.001
∑SAA[2]	22	14.66 ± 0.04	0.66 ± 0.01	21.84 ± 0.67	0.99 ± 0.03
∑EAA[3]		430.02 ± 5.30		480.96 ± 0.59	
∑NEAA[4]		508.00 ± 7.49		558.98 ± 3.67	
∑AA[5]		938.02 ± 12.60		1039.94 ± 3.07	
EAAI[6]		148.85 %		196.80 %	

(Amino acids values were in mg/g of protein).
Values represented as mean ± standard deviation (except for EAAI).
1 Aromatic amino acids: Phe + Tyr.
2 Sulfur amino acids: Cys + Met.
3 Essential aminoacids: Thr + Cys + Val + Met + Ile + Leu + Tyr + Phe + His + Lys + Trp.
4 Non-essential amino acids: Asp + Ser + Glu + Pro + Gly + Ala + Arg.
5 Total amino acids.
6 Essential amino acid index.

Table 2
IVPD and PDCAAS of ACD and ACLP.

Sample	ACD	ACLP
IVPD (%)	70.14 ± 0.69	~100
PDCAAS (%)	46.31	99.29

precipitated protein concentrate was collected by centrifugation (4000 rpm, 15 min) and then freeze-dried for later use. Determination of protein content by BCA method. The yield of the extracted protein was calculated as:

$$\text{Extracted protein yield}\,(\%) = \frac{M_1}{M_2} \times 100$$

Where M_1 is the mass of protein in ACLP (g), and M_2 is the mass of ACD (g).

2.2.1.2. Amino acids composition. The amino acid composition was determined using the as previously described method with slightly modified (Benhammouche et al., 2021). About 50 mg sample (ACD/ACLP) was mixed with 15 mL HCl (6 M) for acid hydrolysis (110 ℃, 24 h), then filtered through 0.22 μm cellulose membrane. Mix amino acid standard working solution (100 nmol/mL) and sample determination solution were injected into the automatic amino acid analyzer (L-8900, Japan) in equal volumes. The amino acid concentration in the sample was calculated by an external standard method using the peak area. Separate determination of tryptophan using alkaline hydrolysis (110 ℃, 18 h). The resulting derivatization of AAs was then subjected to HPLC analysis (Agilent 1260 Infinity II, Germany).

The content of each amino acid in a sample was calculated as follows:

$$X_i = \frac{c_s \times A_i \times F \times V \times M}{A_s \times m \times 10^9} \times 100$$

Where X_i is the amount of amino acid i in the sample (g/100 g), c_s is the amino acid s content of amino acid standard working solution (nmol/mL), A_i is the peak area of amino acid i of the sample determination solution, F is the dilution multiplier, V is the volume of sample hydrolysate transferred for fixing (mL), M is the molar mass of amino acid i (g/mol), A_s is the peak area of amino acid s for an amino acid standard working solution, m is the sample mass (g), 10^9 is the factor that converts the sample content from nanograms (ng) to grams (g), and 100 is the conversion factor.

2.2.1.3. In vitro digestion. The *in vitro* digestion procedure was performed as a previous study (Brodkorb et al., 2019). The routine consists of oral phase, gastric phase and intestinal digestion. Centrifugation after digestion and the precipitate was freeze-dried and analyzed for protein content using Kjeldahl method. *In vitro* protein digestibility (*IVPD*) was calculated as follows:

$$IVPD(\%) = 1 - \frac{\text{undigested protein content in pellet}\,(\text{mg/g})}{\text{initial protein content}\,(\text{mg/g})} \times 100$$

Where undigested protein content in pellet (mg/g) is the amount of protein in the remaining precipitate after the sample has been digested, and initial protein content (mg/g) is the amount of protein in the sample before it has been digested.

2.2.1.4. Estimation of nutritional protein quality. The nutritional protein quality of ACD and ACLP were evaluated according to their essential amino acid (EAA) profile. EAA scores (EAAS) and EAA index (EAAI) were calculated as follows (Benhammouche et al., 2021):

$$EAAS = \frac{a_p}{a_s}$$

$$EAAI(\%) = \sqrt[n]{\frac{Lys_{1p}}{Lys_{1s}} \times \frac{Tyr_{2p}}{Tyr_{2s}} \times \cdots \times \frac{Hist_{np}}{Hist_{ns}}} \times 100$$

Where a is an EAA, p is the test protein, s is the reference protein, and n is the number of amino acids included in the calculation. The reference protein from the WHO/FAO/UNU (2007) EAAS pattern.

The PDCAAS was calculated as:

$$\text{PDCAAS} = \text{Lowest uncorrected amino acid score} \times \text{IVPD}$$

Where *IVPD* is the *in vitro* protein digestibility (%).

2.3. Structural characterization

2.3.1. SDS-PAGE

Referring to Kaur and Bhatia (2022) method with modifications. The sample volume was 15 μL (ACLP solution/loading buffer, 4:1 (v/v)). The concentration of the isolated and concentrated gel was 10 % and 6 % respectively. Samples were electrophoresed at a constant current of 80 mV for 30 min and then 120 mV for 90 min. After electrophoresis, the gel was dyed with Coomassie brilliant blue R-250 (120 min) and decolorized with methanol/glacial acetic acid (v/v 3:1), then imaged (Gel Doc XR + Gel Documentation System, USA).

2.3.2. Sulfhydryl, disulfide bond and surface hydrophobicity analysis

The sulfhydryl, disulfide bond content was determined with reference to the following methods. Two portions of ACLP were dissolved in Tris-Gly buffer (dissolved free sulfhydryl groups) and Tris-Gly-8 M Urea buffer (dissolved total sulfhydryl groups) respectively, then DTNB solution was added before lightproof oscillation (1 h). Finally, the supernatant absorbance at 412 nm was measured after centrifugation (5000 rpm, 10 min). The sulfhydryl content was calculated as follows:

$$\mu\text{molSH/g} = 73.53 \times A_{412} \times D/C$$

Where D is the dilution multiplier, taken as 1.01, C is ACLP concentration (mg/mL), and A_{412} is the absorbance value.

For the disulfide bond testing, mercaptoethanol was added to 0.3 mg/mL of ACLP solution (Tris-Gly-10 M Urea buffer) by 1:16 V/V, the mixture was rested for 1 h (25 ℃) before TCA solution added. After 1 h resting, the solution was centrifuged at 5000 rpm for 10 min, and the obtained precipitation was washed with TCA (3 repetitions). Subsequently, 3 mL Tris-Gly-8 M Urea buffer and 0.04 mL DTNB solution were added and rested for 30 min without light. Finally, the supernatant absorbance at 412 nm was measured after centrifugation (5000 rpm, 10 min), and the disulfide bond content was calculated as follows:

$$\mu\text{molS} - \text{S/g} = (73.53 \times A_{412} \times D/C - SH_{Total})/2$$

Where D is the dilution multiplier, taken as 6.08, C is ACLP concentration (mg/mL), and A_{412} is the absorbance value.

The method of determination of surface hydrophobicity is referenced as follows 10 mg ACLP was dissolved in 40 mL SDS solution, centrifuged (5000 rpm,10 min) after magnetic stirring (4 h), and the supernatant was dialyzed in distilled water for 48 h. Next, 0.25 mL dialysate was mixed with 5 mL of chloroform, then 5 mL of methylene blue solution (0.24 g/L) was added. After centrifugation (2500 rpm, 15 min), the bottom layer of SDS was mixed with methylene blue. The absorbance value at 655 nm was measured. The hydrophobicity of the protein surface was calculated as follows:

$$\text{Surface hydrophobicity} = \frac{\text{Total SDSquality}/\mu\text{g} - \text{Not combined with SDS quality}/\mu\text{g}}{\text{Protein sample quality/mg}}$$

2.3.3. Ultraviolet spectroscopy

UV spectral was referred to the previous method (Du et al., 2018), 1 mg/mL solution of the ACLP was prepared and the absorbance was measured in a quartz cuvette using a UV spectrophotometer with a scan range of 240–320 nm (Metash, China).

2.3.4. FTIR spectroscopy

ACLP infrared spectroscopy detection was based on the Pérez-Vila, Fenelon, Hennessy, O'Mahony, and Gómez-Mascaraque (2023) method. The ACLP (about 1 ~ 2 mg) was mixed with dried KBr (100 mg), ground into a powder, then put into a mould and pressed into a transparent sheet, which was scanned in the infrared spectrometer in the range of 500–4000 cm^{-1} (Thermo Fisher Scientifc, USA).

2.3.5. Circular dichroism

Detection of circular dichroism and analysis of the structural composition of ACLP by the following method. 0.5 mg/mL ACLP solution was prepared and scanned at the speed of 2 nm/s over a 190–260 nm range. The secondary structure of the ACLP was analyzed and calculated using BeStSel (Beta Structure Selection) software.

2.4. Functional features

2.4.1. Protein solubility and zeta-potential

The method for determining protein solubility and zeta-potential were slightly modified according to Fang et al. (2023) study. The protein sample (1 % (m/v) concentration) was adjusted for pH 2 ~ 12 with HCl or NaOH (1 M) and centrifuged (4000 rpm, 20 min) after ultrasonication (20 min), then the protein content of the supernatant was measured using BCA method. ACLP solubility is expressed as a percentage of the total protein concentration in the soluble supernatant. The Zeta-potential (ζ, mV) of ACLP was determined using a nanolaser particle sizer (Nanobrook Omni) at different pH (6 ~ 12) conditions.

2.4.2. Water and oil holding capacity

The water holding capacity (WHC) and oil holding capacity (OHC) of the ACLP were determined based on the method proposed by Ma, Grossmann, Nolden, McClements, and Kinchla (2022) with modifications. After weighing 0.5 g (W_0) ACLP into a centrifuge tube, the total weight of ACLP and centrifuge tube was recorded as W_1, then 10 mL H_2O/soybean oil was added to the tubes and the mixture was left stand for 30 min (25 ℃) before centrifuged (4000 rpm, 10 min). Discarding the supernatant and recording the total weight of the tube and precipitate as W_2, and calculating the WHC and OHC according to the following formula:

$$\mathrm{WHC/OHC} = \frac{W_2 - W_1}{W_0}$$

2.4.3. Foaming capacity and foam stability

The foaming capacity (FC) and foam stability (FS) of the ACLP were determined according to the method proposed by Chalamaiah, Esparza, Temelli, and Wu (2017) method with modified. ACLP solution (2 mg/mL) was stirred for 2 min (10,000 rpm) and then poured into a measuring cylinder, recording the volume of the upper layer of foam and protein solution when stirring stopped, after standing for 30 min, recording the volume of the upper layer of foam again, and calculate the FC and FS according to the following formula:

$$\mathrm{FC} = \frac{V_0}{V_2} \times 100\,;\ \mathrm{FS} = \frac{V_1}{V_0} \times 100$$

Where V_0 is the volume of the upper foam layer when stirring stops (mL), V_1 is the volume of the upper foam layer after stirring has stopped for 30 min (mL), and V_2 is the volume of protein solution at the time of stirring stop (mL).

2.4.4. Emulsifying ability and emulsion stability

Reference to the methodology of Cattan, Patil, Vaknin, Rytwo, Lakemond, and Benjamin (2022) with modifications. 3 mL soybean oil and 9 mL ACLP (2 mg/mL) were homogenized for 2 min (10,000 rpm). 16 μL emulsion from the tube bottom at different time (0 min, 30 min) were mixed with 4 mL of SDS solution (0.1 %) respectively, and then the absorbance value was measured at 500 nm. Emulsifying ability index (EAI) and emulsion stability index (ESI) were calculated according to the following equations:

$$\mathrm{EAI}\left(\frac{m^2}{g}\right) = 2 \times 2.303 \times A_0 \times \frac{D}{c} \times \varnothing \times 1000;\ \mathrm{ESI}\,(\%) = \frac{A_{30}}{A_0} \times 100$$

Where D is the dilution multiple, taken as 125, c is the ACLP concentration (g/mL), ∅ is the volume fraction of the oil phase in the emulsion, taken as 0.25, A_0 and A_{30} are absorbance values at 0, 30 min.

2.5. Antioxidant activities

The *in vitro* antioxidant activities were valued by DPPH radical ($DPPH^+$), hydroxyl radical (·OH), ABTS radical ($ABTS^+$) scavenging activities and reducing power, all these indexes were measured as previously described with several modifications (Sun et al., 2021).

2.6. Statistical analysis

BBD was analyzed and plotted using Design-Expert software (Version 13.0.1) and Origin software (Version 2021). Analysis of variance was studied using ANOVA and means were compared with Duncans new multiple range test with SPSS software (Version 27.0.1). All data were presented as the mean ± SD ($n = 3$). The significance of the differences was defined as the $p < 0.05$.

3. Results and discussion

3.1. Extraction and nutrition quality of ACLP

3.1.1. Chemical composition of defatted ACD

In order to reduce interference of non-polar compounds that may make difficult protein separation by binding to the hydrocarbon chains of some amino acid's residues (Benhammouche et al., 2021), AC was degreased with hexane to obtain ACD for the follow-up study.

The chemical composition of ACD was summarized in Table S1. The protein content (17.57 %) was higher than some other plant materials that were used for leaf proteins extraction previously, such as cabbage (average 3.4 %) (Sedlar, Čakarević, Tomić, & Popović, 2021), bamboo leaves residues (average 12.8 %) (Wang, Harrison, Tonnis, Pinnow, Davis, & Irish, 2018), which suggests a high content of AC protein.

3.1.2. Optimization of protein extraction from ACD

Preliminary study on extracting protein from ACD was carried out by alkaline extraction and acid precipitation. Four factors affecting the ACLP yield were selected and verified one by one. The optimum extraction conditions were shown in Fig. 1A-D, with a material to liquid ratio of 1:30, pH 11, extraction temperature of 40 ℃ and extraction time of 70 min. The experimental results exhibited that the material to liquid ratio, pH, and extraction temperature were the variables of interest for the study, while the extraction time variable had no obvious influence on proteins extraction. Therefore, in the next optimization step, the extraction time was fixed at 70 min.

The three effective independent variables (material to liquid ratio (X_1), pH (X_2), and temperature (X_3)) for extraction of proteins from ACD were optimized using BBD, in order to seek out the best group experimental condition. Using statistically designed experiments, BBD experiments were carried out in a random way under different combinations of these parameters, and the range parameters were shown in Table S2.

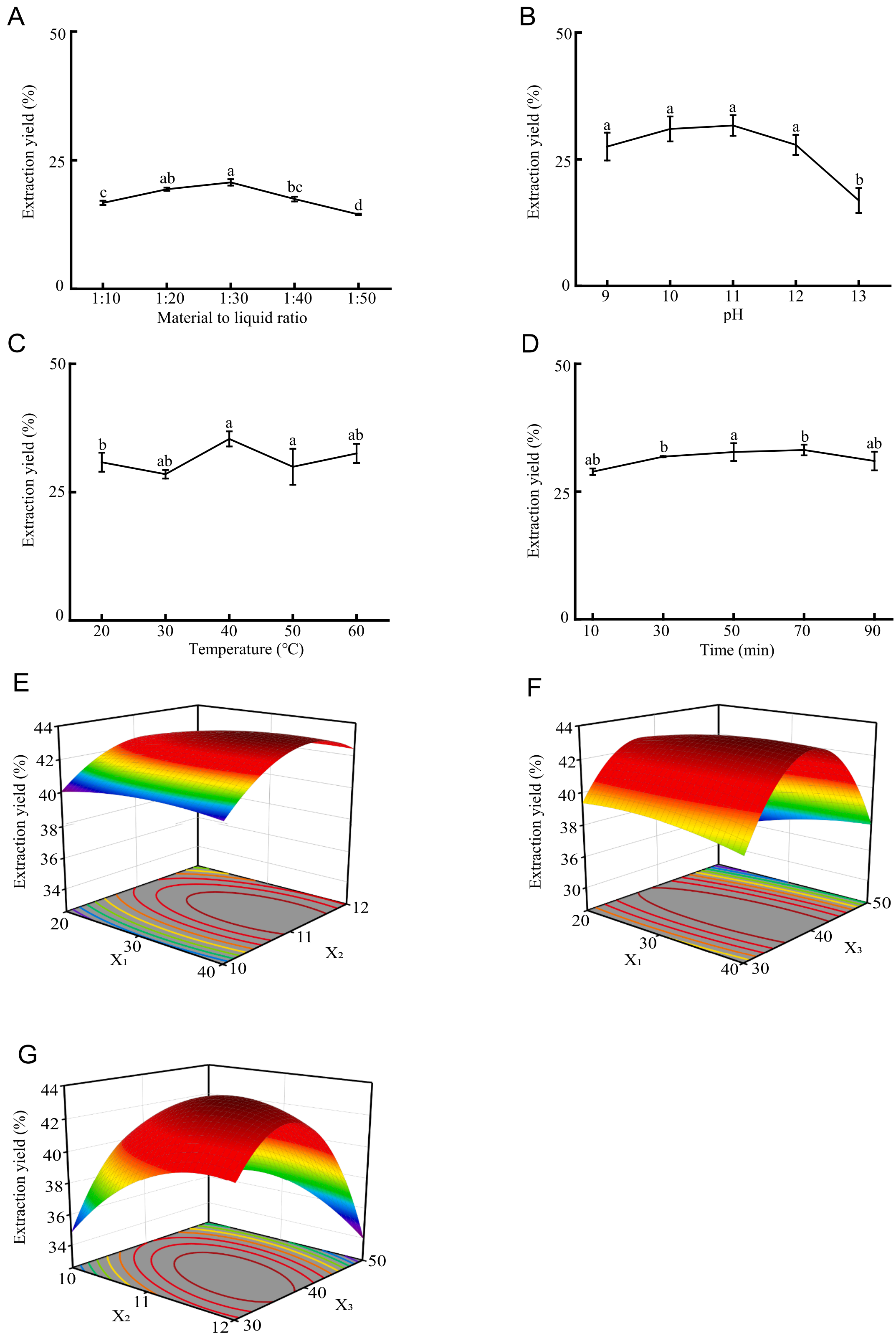

Fig. 1. Effects of main factors on the extraction yield of ACLP, A-Extraction material to liquid ratio, B-Extraction pH, C-Extraction temperature, D-Extraction time, Response surface plots and contour plots (E, F and G) showing the effect of Extraction material to liquid ratio(X_1), Extraction pH (X_2), Extraction temperature (X_3) on ACLP extraction yield. Different letters indicate significantly different ($p < 0.05$).

Performing regression analysis to fit the response function and obtain the final model. The model had good applicability with a model $p < 0.0001$ and values of 0.9976 and 0.9945 for R^2 pred and R^2_{adj} respectively. Therefore, the overall quadratic response surface model was highly significant and meaningful. Multiple regression was fitted to the experimental data in Table S3 using Design-Expert 13 software and the resulting regression equation was $Y = -342.66–0.27 \times X_1 + 49.1 \times X_2 + 5.87 \times X_3 + 0.02 \times X_1 \times X_2 + 0.008 \times X_1 \times X_3 - 0.191 \times X_2 \times X_3 - 0.004 \times X_1^2 - 1.88 \times X_2^2 - 0.05 \times X_3^2$, where X_1 is the material to liquid ratio, X_2 was the pH and X_3 was the extraction temperature.

The response surface and contour plots in Fig. 1E-G can visually reflect the interactive effect between the two factors on the extracted protein yield. The inclination of the spatial surface in the upper part of the figure reflects the degree of influence of the corresponding factor on the response value, while the ellipse eccentricity in the lower part of the contour plot reflects the magnitude of the effect of the interaction between the two factors. The results of the multivariate fitting analysis shown that the optimum extraction process for ACLP was material to liquid ratio 1:31, pH 11.24, and temperature 38.76 ℃. Taking into account the actual situation, the material to liquid ratio was determined as 1:31, pH as 11, and temperature as 39 ℃. The maximum theoretical value of ACLP yield under these conditions was 43.56 %. The measured yield was 43.46 ± 0.68 %, and the validation results were similar to the predicted results. The protein content of ACLP using Kjeldahl method was 42.65 ± 0.03 %.

3.1.3. Amino acid composition

The amino acid (AA) profile, i.e., the content of 18 AAs in ACD was detailed in Table 1. All 18 AAs existed in ACD, Glu and Asp were the first and second most abundant AAs with a concentration of 125.26 ± 1.38 and 103.14 ± 0.96 mg/g protein respectively. As L-Glu and L-Asp are the main flavor AAs that contributed to food taste (Phat, Moon, & Lee, 2016), our results suggest ACLP may be able to enhance food taste and edible value or be used in producing spices. Met was the AA with the lowest concentration (2.13 mg/g protein), which was also the lowest AA in many other plant proteins like the classical plant protein soybean (Sá et al., 2020). In addition, the content of essential AAs (EAAs) (including essential and semi-essential AAs) (430.15 mg/g), aromatic AAs (AAAs) (85.64 mg/g), non-essential AAs (NEAAs) (508.00 mg/g) and total AAs were comparable to or higher than *Moringa Oleifera* defatted (MODL) leaves (Benhammouche et al., 2021), one of the most studied materials for leaf protein. But sulfur AAs (SAAs) concentration (14.66 mg/g) was lower in ACD than MODL. ACLP has a similar amino acid profile with mulberry leaf proteins (MLP), and ACLP has higher AAAs and total AAs than MLP and its six hydrolysates (Sun et al., 2021).

Moreover, the total AAs of ACD and ACLP were more than those of commercially available protein supplements (calcium caseinate powder (CCP), milk protein concentrate powder (MPCP), egg white powder (EWP), pea protein isolate powder (PPIP), whey protein concentrate powder (WPCP) and soy protein isolate powder (SPIP)), which demonstrated higher total AAs than all of the above mentioned commercially available protein supplements, and the ACLP exhibited EAAs comparable to CCP (Corgneau et al., 2019).

Overall, the extraction of ACLP from ACD by alkaline solubilization and acid precipitation had a variable effect on the amino acid profile, with most of the amino acid concentrations increased, especially Trp concentration with an increasing rate of about 5-fold. And the concentration of limited AA Met was also increased more than 3-fold. This means protein extraction resulted in ACLP with a higher AA concentration than ACD.

3.1.4. Amino acid score (AAS) and essential amino acid index (EAAI) for protein quality evaluation

To assess the quality of ACD protein in human nutrition, EAAs was compared with WHO/FAO/UNU, (2007) recommended pattern of EAAs, according to the ratio of EAA in the daily requirement provided by WHO/FAO/UNU, (2007). When the AAS value is less than 1, the relative EAA was regarded as limiting amino acids (LAA). Table 1 demonstrated a comparative overview of the AAS values of ACD and ACLP. The results shown that the AAS values for both ACD and ACLP are within or above the WHO/FAO (AAS ≥ 1) range, except for sulfur amino acids (Cys + Met), which makes sulfur amino acids (Cys + Met) the only LAA, but which had an AAS value of 0.99 ± 0.03 that closely to 1, that was higher than the AAS (Cys + Met = 0.91) of pea protein isolate powder (Corgneau et al., 2019), indicating that ACLP had excellent nutritional value.

In order to investigate the proper balance of EAAs integrity, the EAA index (EAAI) was calculated to evaluate the quality of ACD protein, the high value of EAAI usually indicates a good quality and efficiency of proteins (Yang, Huang, Zhang, Zhang, Huang, & Yang, 2018). In this context, EAAI value of ACD protein (148.85 %) and ACLP (196.80 %) were both higher than 100, which suggested that the ACD and ACLP AA composition was superior to WHO/FAO standard and may perfectly meet WHO/FAO protein quality expectations.

3.1.5. In vitro protein digestibility

As food is a complex mixture of multiple compounds, many factors may interfere with the efficient absorption, digestion, and utilization of protein and reduce protein bioavailability and nutritional status. Plant proteins are usually considered inferior to animal proteins not only for their lack of certain EAAs but also for their gastro-intestinally less bioavailable or less digestible (Sim et al., 2021). The low digestibility of plant protein may be contributed to the following aspects: (1) the high presence of dietary fiber reduces plant proteolytic digestibility; (2) anti-nutritional factors in plants like trypsin inhibitors and phytates may interact with protein hindering digestion and absorption; and (3) plant proteins structure is different from animal proteins, which contains more β-sheet and fewer α-helixes than animal proteins structures predisposing to aggregation (Carbonaro, Maselli, & Nucara, 2012). So, the AAS and composition of the absorbed available AA in a mixture will reflect the relative digestibility of the individual food protein constituents. In order to assess the quality of protein after *in vitro* digestion, the WHO/FAO Expert Coordination Committee proposed the use of the Protein Digestibility Corrected Amino Acid Score (PDCAAS), which takes into account both the least restrictive amino acid score and protein digestibility. Plant proteins often exert low PDCAAS (0.4 ~ 0.9) while animal have high proteins PDCAAS (≥1). In this work, the protein digestibility and PDCAAS of ACD were 70.14 % and 46.31 % respectively (Table 2). When compared to some common grain crops, the PDCAAS of ACD was lower than rice (PDCAAS 53 %) but higher than wheat, pearl millet (PDCAAS 40 %), and sorghum (PDCAAS values as low as 20 %) (Boye, Wijesinha-Bettoni, & Burlingame, 2012). Our results suggested that ACD was a promising protein source for human nutrition and that ACLP obtained through processing has higher protein digestibility (~100 %) and PDCAAS (99.29 %) (Table 2). However, an effective strategy to enhance the protein's nutritional quality by incorporation, fortification or modification needs further study.

3.2. ACLP structure characterization

3.2.1. SDS-PAGE

Structure determines functional properties, and differences in polypeptide size had a direct influence on protein functional properties (Wu et al., 2019). The SDS-PAGE profile of ACLP was shown in Fig. 2A, a single band with a molecular weight of around 25 kDa appeared, which suggests a high homogeneity of ACLP subunit composition. The similar band was also appeared in pea protein isolate (Adebiyi & Aluko, 2011), and radish leaf protein fraction (Kaur & Bhatia, 2022).

3.2.2. Sulfhydryl, disulfide bond, surface hydrophobicity analysis

Sulfhydryl, disulfide bond, and surface hydrophobicity are key factors for protein structure maintenance and functional properties. Sulfhydryl and disulfide bond is the oxidation state and reduction state of

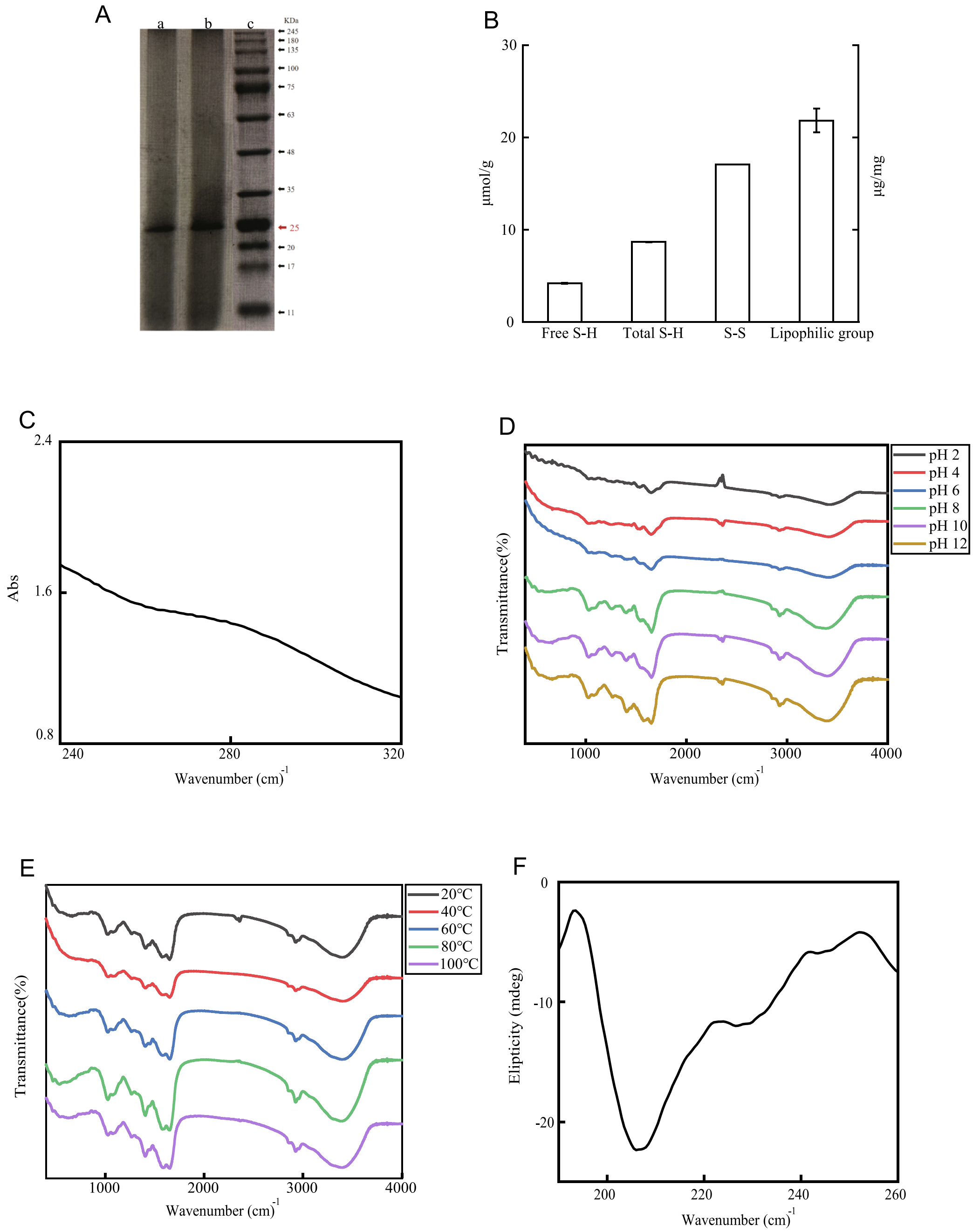

Fig. 2. Structural characteristics of ACLP: A-SDS-PAGE (a-80 mg/mL; b-100 mg/mL; c-Marker), B-Sulfhydryl, disulfide bond, surface hydrophobicity content, C-Ultraviolet spectrum, D-FTIR spectrum (different pH), E-FTIR spectrum (different temperatures), F-Circular dichroism spectroscopy.

free sulfhydryl (Wu et al., 2019), and surface hydrophobicity refers to the number of hydrophobic amino acid restudies on the surface of protein (Uruakpa & Arntfield, 2006). Sulfhydryl, disulfide bond, and surface hydrophobicity are closely related to protein gelation via hydrophobic and disulfide bonds forming, and oxidation and reduction of disulfide bonds could change the protein structure thus modify biology activity (Wu et al., 2019). As shown in Fig. 2B, the free -SH, total -SH contents and -S—S- of ACLP were 4.19 ± 0.03 μmol/g, 8.66 ± 0.02 μmol/g and 17.03 ± 1.27 μmol/g, respectively, means nearly half of the -SH was buried within the interior. The surface hydrophobicity of ACLP was 20.93 ± 2.06 μg/mg, SDS can stretch out the structure of ACLP and its concentration can influence the protein structure and the degree of stretching of the peptide chain of the protein molecule, suggesting several of their hydrophobic residues were away from the hydrophilic environment by being buried within the protein core.

3.2.3. Ultraviolet analysis

Ultraviolet spectra of ACLP in the range of 240 ~ 320 nm was shown in Fig. 2C, which is the characteristic absorption peak of protein. This suggested that the protein in ACD was indeed effectively extracted by the optimized method, obtained ACLP can be used for the following experiment.

3.2.4. FTIR spectrum analysis

FTIR spectroscopy was recognized as a powerful implement for estimating the molecular architecture of proteins and can be used to obtain information of protein structure composition. There are nine amide bands called A, B, and I-VII according to frequency-decreasing order generated by proteins and peptides. The amide band I (1600–1690 cm^{-1}), amide band II (1480–1575 cm^{-1}), and amide band III (1229–1301 cm^{-1}) are generally used to analyze protein structure

(Pérez-Vila et al., 2023). In detail, the amide I band is mainly C═O stretching vibration, which comes from the amide groups weakly united with in-plane NH-bending and CN stretching; the amide II band is primarily an out-of-phase combination of the NH in-plane bend and CN stretching vibration with minor contributions from the CO in-plane bend and CC and NC stretching vibration; while amide III band is an in-phase combination of NH bending and CN stretching vibration with small contributions from CO in-phase bending and CC stretching vibration (Carbonaro & Nucara, 2010). The FTIR spectra of ACLP at different pH were shown in Fig. 2D, and the typical amide I band that can characterize the secondary structure of proteins appeared from 1650.95 cm^{-1} to 1654.01 cm^{-1}. The absorption peaks from 1650 cm^{-1} to 1660 cm^{-1} can indicate the α-helix structure in the proteins, and the peak heights and the peak areas of α-helix regions increased with the increase of pH. This implies that ACLP contains a higher proportion of α-helix at pH 12 compared to pH 2, and α-helix has been reported to be favorable for protein solubility, as it induces a looser protein conformation (Muller, Bernier, & Bazinet, 2023). The FTIR spectra of ACLP at different temperatures were illustrated in Fig. 2E, as the temperature increases, the peak height and peak area at 1574.18 cm^{-1} to 1577.13 cm^{-1} increase, whereas the peak height and peak area at 1651.15 cm^{-1} to 1653 cm^{-1} decrease, which can be speculated that the α-helix is transformed into the β-turn structure and the β-sheet structure of ACLP. High temperature can effectively increase the kinetic energy of protein molecules, leading to the vibration of polar groups, which further causes changes in secondary structure (Li et al., 2022). With increasing temperature, the

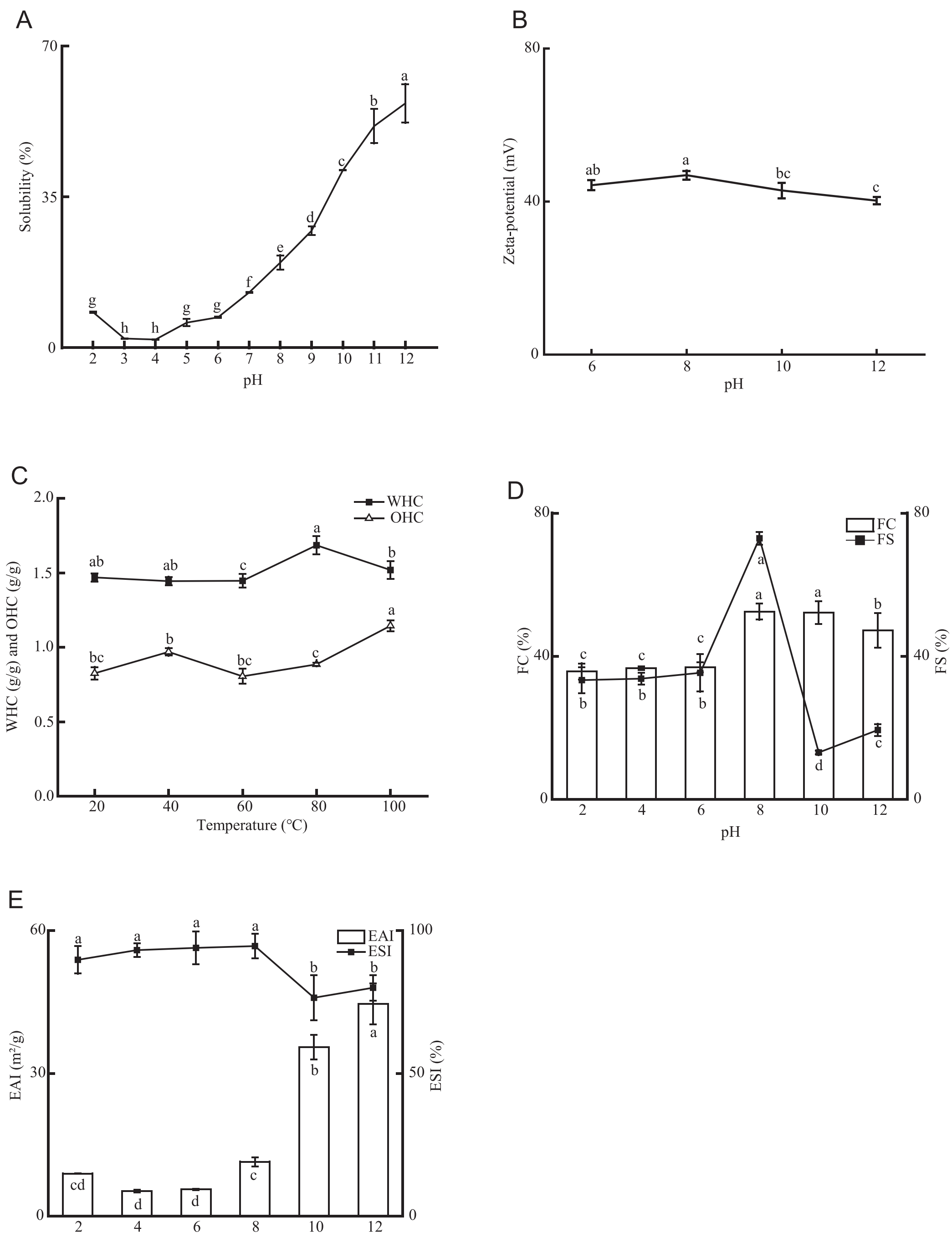

Fig. 3. Functional properties of ACLP: A-Solubility, B- Zeta-potential, C-Water and oil holding capacity (WHC and OHC), D-Foaming and foam stability (FC and FS), E-Emulsifying ability and emulsion stability (EAI and ESI). Different letters indicate significantly different ($p < 0.05$).

peaks in the amide A region (3390.19 cm^{-1} ~ 3399.33 cm^{-1}) were blue shifted, the frequency of the N—H stretching vibration increased, and the intramolecular hydrogen bonding structure was changed.

3.2.5. Circular dichroism spectroscopy

CD spectroscopy has been extensively harnessed to discern the secondary structure of proteins. CD spectroscopy of ACLP in the far UV region from 190 to 260 nm was investigated. As can be seen from Fig. 2F, the negative ellipticity around 208 nm belongs to the $\pi \rightarrow \pi^*$ transition was attributed the structure of α-helix. And the positive ellipticity around 195 nm and the negative ellipticity around 216 nm indicated β-sheet structure in ACLP. Further, the software BeStSel (Beta Structure Selection) was used to fitting the secondary structure and the result suggested there were about 2.3 % α-helix, 29.7 % β-sheet, 14.7 % β-turn, and 53.3 % random coil in the ACLP secondary structure. The high content of disordered structure perhaps was related to the alkaline extraction which may disrupted peptide's structure and hydrogen bonds thus affecting the stability of the α-helical and β-sheet structures in ACLP.

3.3. Functional properties of ACLP

3.3.1. Protein solubility and Zeta-potential

Solubility is an important prerequisite for protein to be used in food, which indicates the ability of protein to dissolve in solvents. In thermodynamics, solubility is the manifestation of the equilibrium between protein–protein and protein-solvent interactions under a given condition, which is directly associated with the physicochemical nature of the protein surface and can indirectly reflect the changes in the structure, balance of charge, and hydrophobicity of the protein molecule (Nakai, 1983).

Fig. 3A shown the pH-dependent solubility profile of ACLP, ACLP solubility was lower from pH 2 to 4, while increased from pH 4 as the pH increased, which was akin to the solubility profile reported for hemp protein isolate (Fang et al., 2023). The poor solubility of ACLP may be caused by the high content of hydrophobic amino acid (39.72 %) and glutamic acid (13.35 %). The minimum solubility was obtained at pH 4 and the maximum solubility at pH 12 or higher (not tested). pH 4 may be around the isoelectric point (pI) of ACLP, under which the hydrophobic interactions between proteins are much larger than hydrophilic and hydration repulsive force leading to protein aggregation and precipitation. The higher solubility in alkaline pH may be caused by the increase of net protein charge with the increase of pH value, this was verified in Fig. 3B. The Zeta-potential of ACLP was increased with pH elevating, the pH-dependent solubility curve shown a good correlation with the Zeta-potential of protein. Besides, the changes in pH-dependent solubility were also consistent with the structure changes in Fig. 2D. These results suggested the suitable application of ACLP in alkaline foods, but the pH higher than 10 was not satisfactory in food processing because of inadvisable reaction which could impact food quality and safety. So, research on improving solubility of ACLP should be focused and is vital for its widespread application in food.

3.3.2. Water and oil holding capacity

WHC and OHC mean how much water or oil can a unit weight of protein hold. WHC and OHC reflect protein's ability to prevent liquid loss from products during processing or storage in protein, which is closely related to food flavor and texture (Ma et al., 2022).

The temperature-dependent WHC and OHC profile of ACLP depicted that ACLP WHC was at least 1.44 ± 0.03 g/g from 20 °C to 100 °C (Fig. 3C), which is better than *Moringa oleifera* seed protein isolate (0.78 g/g) (Aderinola, Alashi, Nwachukwu, Fagbemi, Enujiugha, & Aluko, 2020). Though the highest was 1.69 ± 0.06 g/g at temperature 80 °C, it was considerably lower than commercially available pulse protein isolates (2.20 ~ 7.57 g/g). This may be to some degree due to the high content of hydrophobic amino acid (39.72 %) in ACLP, as WHC was correlated with AA composition, protein conformation, and the ratio of surface polarity to hydrophobicity. As the temperature increases, the internal structure of the protein unfolds, thus more intramolecular and intermolecular hydrophilic groups could combine with water. High protein WHC is a key criterion for use in viscous foods like soups, confectionery, and bakery products (Du et al., 2018).

In addition, OHC is a critical factor for the retention of flavor in food, fat is mainly bond by nonpolar side chains of protein. The OHC of ACLP was between 0.81 ± 0.05 ~ 1.14 ± 0.04 g/g (Fig. 3C), which was higher than several vegetable leaves proteins concentrate (Sedlar et al., 2021) and comparable to some commercial pulse proteins (Ma et al., 2022). And the OHC was increased when the temperature elevated, may be high temperature broke the nature structure leading more hydrophilic groups exposed, which was implied by the blue shift of amide A region and the secondary conformation changes among α-helix, β-turn structure and β-sheet (Fig. 2D). These results suggested that ACLP can be used in foods like sausages, salad dressings, comminuted meats as meat extenders, flavor retainers and stabilization agents.

3.3.3. Foaming capacity (FC) and foam stability (FS)

Foam formation is one requirement for the production of food like cake, bread, ice cream. Protein is characteristic of amphipathic which makes them forming interfacial protein membranes at the air–water interface to prevent bubble coalescence. FC depends mainly on the solubility of the protein solution, the number of hydrophobic groups, and the flexibility of the peptide chain, while the FS depends on the protein's ability to form a cohesive network on the interface through covalence and noncovalent interactions (Chalamaiah et al., 2017). As shown in Fig. 3D, the foaming properties of ACLP was greatly affected by pH, presenting a bell-shaped curve as pH increased with a maximum FC (52.49 %) and FS (72.98 %) at pH 8, which was higher than the FC (20.4 %) and FS (34 %) of some plant proteins like radish leaf protein concentrates (Kaur & Bhatia, 2022). As the pH increased, more loosen structure such as random coil structure was formed in protein (Fig. 2D), which favored its diffusion at the gas–liquid interface to foaming. The continuing increase in pH could reinforce the intermolecular repulsion, which was unfavorable for the protein–protein interaction and the adhesion of protein on the bubble film, resulting in the deterioration of FS. Therefore, ACLP has shown great potential as a foaming ingredient and whipping agent in baked goods, beverages and ice cream.

3.3.4. Emulsifying ability and emulsion stability

The emulsifying property is another important interfacial property of protein means its capacity to react with and stabilize oil–water mixture, which could prevent phase separation (Du et al., 2018). The EAI is the maximum surface area produced per unit of protein, which is often used to express the emulsifying ability. And ESI measures protein's ability to form a stable emulsion within a specified time (Du et al., 2018). As exhibited in Fig. 3E, ACLP depicted the lowest EAI (5.34 m^2/g) at pH 4.0, this may be caused by the lowest solubility around the isoelectric point, but it was still higher than *Moringa oleifera* seed protein extract (Cattan et al., 2022). And EAI increased as pH increased, the highest EAI (44.62 m^2/g at pH 12) was comparable to soy protein isolates (Wang, Tang, Li, Yang, Li, & Ma, 2008), suggesting a positive correlation between emulsification ability and solubility. As the pH increased, more protein side chains dissociated, creating electrostatic repulsive forces (Fig. 3B) that not only favored emulsification system stability but also avoided droplet aggregation. In addition, the protein solubility and hydration capacity were increased when pH had deviated from the pI (Fig. 3A and 3C), which improved the stability of protein film and therefore favored emulsification system stabilization. The lowest ESI of ACLP was 76.53 % at pH 10, which was even higher than ESI of some proteins like hemp protein isolate (Fang et al., 2023), and radish leaf protein concentrates (Kaur & Bhatia, 2022). Higher EAI and ESI of ACLP suggested its good emulsion property and can be used to stabilize emulsions in food products.

3.4. Antioxidant activity

Free radicals are highly reactive species that often induce harmful reactions affecting food quality and nutrition. Moreover, overloading free radical induced oxidative stress is regarded as the cause of various diseases. So, antioxidants especially natural derived compounds have drawn attention for their role in inhibiting oxidative reactions. Leaf proteins or hydrolysates also have been exploited as good potential antioxidants (Calderón-Chiu et al., 2021; Sun et al., 2021).

The antioxidant activities of ACLP and its digested products were analyzed by measuring the free radical ($DPPH^+$, $ABTS^+$ cation, hydroxyl radical) scavenging activity and reducing power. As shown in Fig. 4A, the free radical scavenging abilities and reducing power of ACLP were dose-dependent. The maximum $DPPH^+$ scavenging activity (70.50 ± 0.15 %) of ACLP was about three-quarters of the control Vitamin C under the same concentration (0.2 mg/mL). It worth nothing that the best $ABTS^+$ radical scavenging ability (100 %) of ACLP was comparable to Vitamin C. Differences in radical quenching efficiency may be due to the solubility of radicals and diffusivity. $ABTS^+$ is a water-soluble monocationic radical while $DPPH^+$ is an oil-soluble free radical. $DPPH^+$ was dissolved in ethanol before used, so it may not diffuse to ACLP as easily as $ABTS^+$ since the analysis is conducted in aqueous solution. The ·OH radical scavenging ability of ACLP was superior to Vitamin C when the concentration was lower than 0.1 mg/mL concentration, but the situation was reversed when the concentration was above 0.1 mg/mL. The reducing power of ACLP was totally weaker than

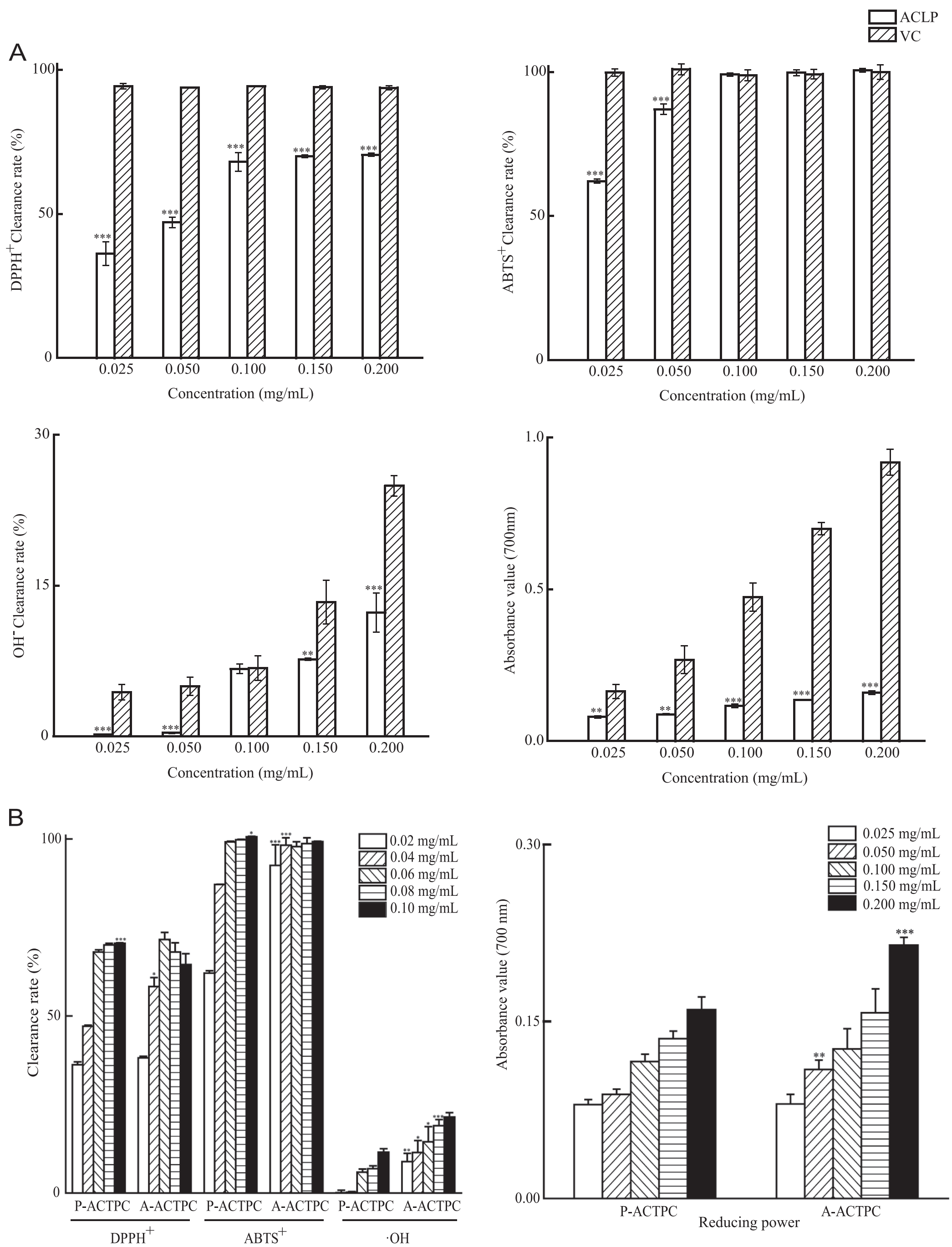

Fig. 4. Antioxidant activity: A-Antioxidant activity of ACLP (compared to Vitamin C), B-Comparison of antioxidant activity and reducing properties of ACLP before and after digestion. * means a significant difference versus control groups (* means $p < 0.05$, ** means $p < 0.01$, *** means $p < 0.001$).

that of Vitamin C at the tested concentration, but it was dose-dependent and had a huge potential for improvement when the concentration increased. The antioxidant capacity of ACLP at 0.2 mg/mL was comparable to or even better than that of mulberry leaf protein at 0.8 mg/mL (Sun et al., 2021). At a sample concentration of 0.1 mg/mL, the free radical scavenging rate of ACLP for $DPPH^+$ and $ABTS^+$ was twice that of Jackfruit leaf protein at the concentration of 0.1 mg/mL for $DPPH^+$ and 1 mg/mL for $ABTS^+$ (Calderón-Chiu et al., 2021). The results suggested ACLP had a potential for acting as antioxidant additives in food industry.

Dietary protein will be digested after ingested and the digestion could change its activity. As shown in Fig. 4B, the free radical quenching abilities and reducing capacity of ACLP digestion products were almost superior to undigested ACLP under the series concentrations. This may attribute to the enzymatic disruption of the protein structure that released lots hydrophobic peptides and exposed more antioxidant bioactive sites. But the $DPPH^+$ scavenging activity was decreased after digestion at 0.1 mg/mL, this may associate with the diffusivity of radicals in reaction medium. As $DPPH^+$ was oil-soluble, the enzyme hydrolysis digested ACLP into more hydrophobic water-soluble peptides and amino acids, and the increased polarity may make it more difficult to capture $DPPH^+$, especially obvious at high concentration.

4. Conclusion

Protein concentrate was extracted from ACD by BBD optimized alkaline extraction and acid precipitation method (material to liquid ratio 1:31, pH 11.24, and temperature 38.76 ℃). ACLP nutrition quality meet the WHO/FAO/UNU, (2007) protein quality expectations. ACLP subunit had high homogeneity with about 25 kDa molecular size, and random coil was the mainly secondary structure while β-sheet conformation was dominant regular conformation. ACLP solubility suggested it may not suitable for acid food application, but it had excellent emulsion ability and foaming capacity. ACLP had antioxidant activity, which was better after digestion. Though there are still many problems need further study to dissolve, our results imply that ACLP could be used as a promising alternative source of protein and food ingredient. Furthermore, more investigate such as *in vivo* metabolic pathway of ACLP need to be done to evaluate its function and side effects on human health.

CRediT authorship contribution statement

Wen-Lu Wei: Writing – review & editing, Supervision. **Wen-Jun Wang:** Supervision, Writing – review & editing. **Hui Chen:** Formal analysis, Data curation. **Su-Yun Lin:** Formal analysis, Data curation. **Qiu-Shui Luo:** Methodology, Formal analysis. **Jian-Ming Li:** Methodology, Formal analysis. **Jin Yan:** Methodology, Formal analysis. **Ling-Li Chen:** Writing – review & editing, Supervision, Methodology, Funding acquisition.

Declaration of competing interest

The authors declare that they have no known competing financial interests or personal relationships that could have appeared to influence the work reported in this paper.

Data availability

Data will be made available on request.

Acknowledgments

The authors gratefully acknowledge the financial supports by Science and Technology Research Projects of the Education Department of Jiangxi Province (GJJ200434).

Appendix A. Supplementary data

Supplementary data to this article can be found online at https://doi.org/10.1016/j.fochx.2024.101153.

References

Adebiyi, A. P., & Aluko, R. E. (2011). Functional properties of protein fractions obtained from commercial yellow field pea (Pisum sativum L.) seed protein isolate. *Food Chemistry, 128*(4), 902–908. https://doi.org/10.1016/j.foodchem.2011.03.116

Aderinola, T. A., Alashi, A. M., Nwachukwu, I. D., Fagbemi, T. N., Enujiugha, V. N., & Aluko, R. E. (2020). In vitro digestibility, structural and functional properties of Moringa oleifera seed proteins. *Food Hydrocolloids, 101*, Article 105574. https://doi.org/10.1016/j.foodhyd.2019.105574

Benhammouche, T., Melo, A., Martins, Z., Faria, M. A., Pinho, S. C. M., Ferreira, I. M. L. P. V. O., & Zaidi, F. (2021). Nutritional quality of protein concentrates from Moringa Oleifera leaves and in vitro digestibility. *Food Chemistry, 348*, Article 128858. https://doi.org/10.1016/j.foodchem.2020.128858

Boye, J., Wijesinha-Bettoni, R., & Burlingame, B. (2012). Protein quality evaluation twenty years after the introduction of the protein digestibility corrected amino acid score method. *British Journal of Nutrition, 108*(S2), S183–S211. https://doi.org/10.1017/S0007114512002309

Brodkorb, A., Egger, L., Alminger, M., Alvito, P., Assunção, R., Ballance, S., Bohn, T., Bourlieu-Lacanal, C., Boutrou, R., Carrière, F., Clemente, A., Corredig, M., Dupont, D., Dufour, C., Edwards, C., Golding, M., Karakaya, S., Kirkhus, B., Le Feunteun, S., & Recio, I. (2019). INFOGEST static in vitro simulation of gastrointestinal food digestion. *Nature Protocols, 14*(4), 991–1014. https://doi.org/10.1038/s41596-018-0119-1

Cai, Y., Zheng, Q., Sun, R., Wu, J., Li, X., & Liu, R. (2020). Recent progress in the study of Artemisiae Scopariae Herba (Yin Chen), a promising medicinal herb for liver diseases. *Biomedicine & Pharmacotherapy, 130*, Article 110513. https://doi.org/10.1016/j.biopha.2020.110513

Calderón-Chiu, C., Calderón-Santoyo, M., Herman-Lara, E., & Ragazzo-Sánchez, J. A. (2021). Jackfruit (Artocarpus heterophyllus Lam) leaf as a new source to obtain protein hydrolysates: Physicochemical characterization, techno-functional properties and antioxidant capacity. *Food Hydrocolloids, 112*, Article 106319. https://doi.org/10.1016/j.foodhyd.2020.106319

Carbonaro, M., Maselli, P., & Nucara, A. (2012). Relationship between digestibility and secondary structure of raw and thermally treated legume proteins: A Fourier transform infrared (FT-IR) spectroscopic study. *Amino Acids, 43*(2), 911–921. https://doi.org/10.1007/s00726-011-1151-4

Carbonaro, M., & Nucara, A. (2010). Secondary structure of food proteins by Fourier transform spectroscopy in the mid-infrared region. *Amino Acids, 38*(3), 679–690. https://doi.org/10.1007/s00726-009-0274-3

Cattan, Y., Patil, D., Vaknin, Y., Rytwo, G., Lakemond, C., & Benjamin, O. (2022). Characterization of Moringa oleifera leaf and seed protein extract functionality in emulsion model system. *Innovative Food Science & Emerging Technologies, 75*, Article 102903. https://doi.org/10.1016/j.ifset.2021.102903

Chalamaiah, M., Esparza, Y., Temelli, F., & Wu, J. (2017). Physicochemical and functional properties of livetins fraction from hen egg yolk. *Food Bioscience, 18*, 38–45. https://doi.org/10.1016/j.fbio.2017.04.002

Corgneau, M., Gaiani, C., Petit, J., Nikolova, Y., Banon, S., Ritié-Pertusa, L., Le, D. T. L., & Scher, J. (2019). Nutritional quality evaluation of commercial protein supplements. *International Journal of Food Science & Technology, 54*(8), 2586–2594. https://doi.org/10.1111/ijfs.14170

Du, M., Xie, J., Gong, B., Xu, X., Tang, W., Li, X., Li, C., & Xie, M. (2018). Extraction, physicochemical characteristics and functional properties of Mung bean protein. *Food Hydrocolloids, 76*, 131–140. https://doi.org/10.1016/j.foodhyd.2017.01.003

Fang, B., Chang, L., Ohm, J.-B., Chen, B., & Rao, J. (2023). Structural, functional properties, and volatile profile of hemp protein isolate as affected by extraction method: Alkaline extraction–isoelectric precipitation vs salt extraction. *Food Chemistry, 405*, Article 135001. https://doi.org/10.1016/j.foodchem.2022.135001

Hadidi, M., Hossienpour, Y., Nooshkam, M., Mahfouzi, M., Gharagozlou, M., Aliakbari, F. S., Aghababaei, F., & McClement, D. J. (2023). Green leaf proteins: A sustainable source of edible plant-based proteins. *Critical Reviews in Food Science and Nutrition, 1–18*. https://doi.org/10.1080/10408398.2023.2229436

Kaur, G., & Bhatia, S. (2022). Radish leaf protein concentrates: Optimization of alkaline extraction for production and characterization of an alternative plant protein concentrate. *Journal of Food Measurement and Characterization, 16*(4), 3166–3181. https://doi.org/10.1007/s11694-022-01411-4

Li, X., Deng, Y., Qiu, W., Feng, Y., Jin, Y., Deng, S., Tao, N., & Jin, Y. (2022). Alteration of collagen thermal denaturation, structural and the abrogation of allergenicity in eel skin induced by ohmic heating. *Food Chemistry, 391*, Article 133272. https://doi.org/10.1016/j.foodchem.2022.133272

Ma, K. K., Grossmann, L., Nolden, A. A., McClements, D. J., & Kinchla, A. J. (2022). Functional and physical properties of commercial pulse proteins compared to soy derived protein. *Future Foods, 6*, Article 100155. https://doi.org/10.1016/j.fufo.2022.100155

Muller, T., Bernier, M.-È., & Bazinet, L. (2023). Optimization of water lentil (Duckweed) leaf protein purification: identification, structure, and foaming properties. *Foods, 12*(18), 3424. https://doi.org/10.3390/foods12183424

Nakai, S. (1983). Structure-function relationships of food proteins: With an emphasis on the importance of protein hydrophobicity. *Journal of Agricultural and Food Chemistry, 31*(4), 676–683. https://doi.org/10.1021/jf00118a001

Pasrija, D., & Sogi, D. S. (2022). Extraction optimization and functional properties of muskmelon seed protein concentrate. *Journal of Food Measurement and Characterization, 16*(5), 4137–4150. https://doi.org/10.1007/s11694-022-01523-x

Pérez-Vila, S., Fenelon, M. A., O'Mahony, J. A., & Gómez-Mascaraque, L. G. (2022). Extraction of plant protein from green leaves: Biomass composition and processing considerations. *Food Hydrocolloids, 133*, Article 107902. https://doi.org/10.1016/j.foodhyd.2022.107902

Pérez-Vila, S., Fenelon, M., Hennessy, D., O'Mahony, J. A., & Gómez-Mascaraque, L. G. (2023). Impact of the extraction method on the composition and solubility of leaf protein concentrates from perennial ryegrass (Lolium perenne L.). *Food Hydrocolloids, 147*, Article 109372. https://doi.org/10.1016/j.foodhyd.2023.109372

Phat, C., Moon, B., & Lee, C. (2016). Evaluation of umami taste in mushroom extracts by chemical analysis, sensory evaluation, and an electronic tongue system. *Food Chemistry, 192*, 1068–1077. https://doi.org/10.1016/j.foodchem.2015.07.113

Pirie, N. W. (1942). Green leaves as a source of proteins and other nutrients. *Nature, 149*(3774), 251.

Sá, A. G. A., Moreno, Y. M. F., & Carciofi, B. A. M. (2020). Plant proteins as high-quality nutritional source for human diet. *Trends in Food Science & Technology, 97*, 170–184. https://doi.org/10.1016/j.tifs.2020.01.011

Sedlar, T., Čakarević, J., Tomić, J., & Popović, L. (2021). Vegetable by-products as new sources of functional proteins. *Plant Foods for Human Nutrition, 76*(1), 31–36. https://doi.org/10.1007/s11130-020-00870-8

Sim, S. Y. J., Srv, A., Chiang, J. H., & Henry, C. J. (2021). Plant proteins for future foods: A roadmap. *Foods, 10*(8), 1967. https://doi.org/10.3390/foods10081967

Sun, C., Shan, Y., Tang, X., Han, D., Wu, X., Wu, H., & Hosseininezhad, M. (2021). Effects of enzymatic hydrolysis on physicochemical property and antioxidant activity of mulberry (Morus atropurpurea Roxb.) leaf protein. *Food Science & Nutrition, 9*(10), 5379–5390. https://doi.org/10.1002/fsn3.2474

Uruakpa, F. O., & Arntfield, S. D. (2006). Surface hydrophobicity of commercial canola proteins mixed with κ-carrageenan or guar gum. *Food Chemistry, 95*(2), 255–263. https://doi.org/10.1016/j.foodchem.2005.01.030

Wang, M. L., Harrison, M. L., Tonnis, B. D., Pinnow, D., Davis, J., & Irish, B. M. (2018). Total leaf crude protein, amino acid composition and elemental content in the USDA-ARS bamboo germplasm collections. *Plant Genetic Resources: Characterization and Utilization, 16*(2), 185–187. https://doi.org/10.1017/S1479262117000053

Wang, X.-S., Tang, C.-H., Li, B.-S., Yang, X.-Q., Li, L., & Ma, C.-Y. (2008). Effects of high-pressure treatment on some physicochemical and functional properties of soy protein isolates. *Food Hydrocolloids, 22*(4), 560–567. https://doi.org/10.1016/j.foodhyd.2007.01.027

WHO, FAO, & UNU (Eds.). (2007). *Protein and amino acid requirements in human nutrition: Report of a joint WHO/FAO/UNU Expert Consultation; [Geneva, 9 - 16 April 2002]*. WHO.

Wu, D., Wu, C., Wang, Z., Fan, F., Chen, H., Ma, W., & Du, M. (2019). Effects of high pressure homogenize treatment on the physicochemical and emulsifying properties of proteins from scallop (Chlamys farreri). *Food Hydrocolloids, 94*, 537–545. https://doi.org/10.1016/j.foodhyd.2019.04.003

Wu, M., Cao, Y., Lei, S., Liu, Y., Wang, J., Hu, J., Li, Z., Liu, R., Ge, Q., & Yu, H. (2019). Protein structure and sulfhydryl group changes affected by protein gel properties: Process of thermal-induced gel formation of myofibrillar protein. *International Journal of Food Properties, 22*(1), 1834–1847. https://doi.org/10.1080/10942912.2019.1656231

Yang, F., Huang, X., Zhang, C., Zhang, M., Huang, C., & Yang, H. (2018). Amino acid composition and nutritional value evaluation of Chinese chestnut (Castanea mollissima Blume) and its protein subunit. *RSC Advances, 8*(5), 2653–2659. https://doi.org/10.1039/C7RA13007D

Yang, Q., Wu, X., Pan, Z., Guan, R., Yang, P., Liu, Y., Yang, X., Du, W., Liang, J., Hu, J., Cai, W., & Ma, G. (2023). Integration of pharmacodynamics, network pharmacology and metabolomics to elucidate effect and mechanism of Artemisia capillaris Thunb. In the treatment of jaundice. *Journal of Ethnopharmacology, 303*, Article 115943. https://doi.org/10.1016/j.jep.2022.115943

Zhang, W., Grimi, N., Jaffrin, M. Y., Ding, L., & Tang, B. (2017). A short review on the research progress in alfalfa leaf protein separation technology: A short review on the research progress in alfalfa leaf protein separation technology. *Journal of Chemical Technology & Biotechnology, 92*(12), 2894–2900. https://doi.org/10.1002/jctb.5364